

# Neurofibromatosis revisited: A pictorial review

**Nausheen Khan, MB BS, FCRad (D) SA**

**Irma van de Werke, MB BCH, DMRD, FRCR**

Department of Radiology, Kalafong Hospital, University of Pretoria

**Farzanah Ismail, MB BCH**

Department of Radiology, Steve Biko Academic Hospital, University of Pretoria

Because of the large number of images accompanying this review, and the cost of including them in the printed version of the journal, only the text has been published in print while the full review with all images appears on the open-access SAJR website <http://www.sajr.org.za>. Go to the site, click on Current, then on the image of this issue's front cover, and then on the title of this review on the contents page.

## Abstract

Neurofibromatosis (or von Recklinghausen disease) is a hereditary condition due to mesodermal and neuroectodermal dysplasia, eponymously named after the researcher who reported it in 1882. The disorder is transmitted as an autosomal dominant condition, but 50% of cases arise as spontaneous mutations. The incidence falls within the range 1:2 000 - 1:4 000, and has no gender bias. We present a series of images produced by different modalities that show lesions and pathologies that are characteristic of the disease.

## Introduction

Despite being named after von Recklinghausen, who documented the disorder in 1882, the classical signs of neurofibromatosis were first reported by Smith in Dublin in 1849.<sup>1</sup> Neurofibromatosis represents a form of disseminated phakomatosis.<sup>1</sup> The term 'phakoma' (from the Greek *phakos* – lentil) is used for a lentil-shaped object such as a mark on the skin or the retina.<sup>2</sup> The disorder is transmitted as an autosomal dominant condition, but 50% of cases arise as spontaneous mutations. There is no gender predilection.<sup>3</sup>

Neurofibromatosis is not a single entity but actually a group of heterogeneous diseases. Although several variants of neurofibromatosis have been proposed, only 2 distinct types have been defined to date. Neurofibromatosis type 1 (NF1) is also termed peripheral neurofibromatosis, and neurofibromatosis type 2 (NF2) as central neurofibromatosis, due to their more peripheral and central involvement, respectively. Because NF1 often has central lesions and NF2 can occasionally have peripheral manifestations, the terms central and peripheral have been discarded.<sup>4</sup> Segmental neurofibromatosis (NF5) is a rare form of neurofibromatosis in which the cutaneous and neural changes are confined to one region of the body. Pain and pruritis (due to the large number of

mast cells in the neurofibromas) are the presenting symptoms in most afflicted patients. The genetics and the relationship of segmental neurofibromatosis to von Recklinghausen disease is undetermined.<sup>4</sup>

The classic clinical signs include cutaneous pigmentation (café au lait) spots, multiple soft tissue tumours (molluscum fibrosum) and palpable neurofibromas of the peripheral nerves.<sup>3</sup>

## Neurofibromatosis type 1 (NF1)

NF1 is the most common of the phakomatoses. It is an autosomal dominant condition with high penetrance and abnormalities localised to the pericentrometric region of chromosome 17, with 50% having spontaneous mutants with variable expressivity. The incidence is 1:2 000 - 4 000 with a male:female ratio of 1:1. Mental retardation is present in 10% of cases.

### Diagnostic criteria<sup>4,5</sup>

Diagnosis of NF1 is established when 2 or more of the following are present:

- 6 or more café au lait spots  $\geq 5$  mm
- 1 plexiform neurofibroma or more neurofibromas of any type
- $\geq 2$  pigmented iris hamartomas (Lisch nodules)
- freckling in the axillary or inguinal regions
- optic nerve glioma
- first-degree relative with NF
- presence of a characteristic bone lesion (e.g. dysplasia of greater wing of sphenoid, pseudoarthrosis).

MR imaging findings have not at present been incorporated into the diagnostic criteria.

## Radiological presentation

### Skull, meningeal and osseous lesions

The most common abnormality of the skull includes macrocrania, hypoplasia of the greater wing of the sphenoid (harlequin appearance of the orbit) (Fig. 1) with temporal lobe herniation into the orbit (buphthalmos), calvarial defects (lambdoid and, uncommonly, coronal suture) (Fig. 2a - d), and dural ectasia.<sup>4</sup>

Enlargement of the internal auditory canal in NF1 that is sometimes seen, is usually the result of dural ectasia and is not due to acoustic neuromas.<sup>4</sup>

### Orbits and brain

Optic nerve gliomas (ONGs) are seen in 5 - 15% of cases, can involve one or both optic nerves and commonly extend posteriorly to involve the chiasma (Fig. 3a - c). Posterior involvement of the optic tracts and radiation and lateral geniculate body is less commonly seen. Study by Kornreich *et al.* concluded that the most common site of involvement was the orbital nerve (66%), followed by the chiasma (62%). In patients who do not have NF, the chiasma is the most common site of involvement (92%).<sup>5</sup> Most ONGs are benign, but 20% of chiasmatic gliomas in

children may behave aggressively.<sup>4</sup>

Imaging is best determined by magnetic resonance imaging (MRI). Most tumours are iso- to hypo-intense to brain on T1 (Fig. 3b) and show increased signal on T2 (Fig. 3c). There is variable post-intravenous contrast enhancement. Imes *et al.* have reviewed the MRI findings in 4 patients with ONG and have found that double-intensity tubular thickening characteristic of perineural arachnoidal gliomatosis, elongation of the nerves and downward kinking of the nerves in the mid-orbit are typical imaging findings on MRI.<sup>6</sup>

Non-optic gliomas have an increased frequency of occurrence in NF1. Most are low-grade benign astrocytomas of the brain stem, tectum and periaqueductal region.<sup>4</sup> Plexiform neurofibromas are a hallmark of NF1 and are diagnostic of von Recklinghausen NF (Fig. 4). They are found in about a third of patients with NF1.

Plexiform neurofibromas are poorly delineated diffusely infiltrating multiple tortuous worm-like masses (Fig. 5a) that arise along the axis of the major nerves. The first division (orbital) of the trigeminal nerve (Fig. 5b) is commonly involved and often associated with sphenoid wing dysplasia and middle cranial fossa arachnoid cyst or prominent subarachnoid space.<sup>4</sup>

A computed tomography (CT) scan shows a poorly defined mass in the infratemporal fossa (Fig. 4). On MR imaging, plexiform neurofibromas are isointense to muscle on T1 and enhance moderately to intensely on post-contrast images. Sarcomatous change is reported in 5 - 15% of cases.

Benign brain parenchymal abnormalities are observed in nearly 80% of patients with NF1. Multiple lesions in the basal ganglia, optic radiation, brain stem and cerebral peduncles are common. On CT scan, they are seen as relatively well-defined unilateral or bilateral hypodense lesions with no appreciable mass effect or contrast enhancement (Fig. 6a). On MRI, they appear as focal areas of signal intensity (FAWI) in white matter and deep grey matter.<sup>7</sup> The lesions are of variable intensity on T1-weighted images and are hyperintense on T2-weighted images, with sharp or hazy margins. Pathologically, these lesions are foci of hyperplastic or dysplastic glial proliferation, and not neoplastic, and do not show mass effect or contrast enhancement (Fig. 6b - d). These white-matter changes usually diminish with age.<sup>4</sup> Lesion progression in a child >10 years of age warrants close follow-up to rule out neoplasm.<sup>8</sup>

### Spine (spinal cord and nerve roots)

The incidence of spinal involvement in NF1 is approximately 60%. In a study of patients with NF1 by Thakkar *et al.*, 6% of patients had intramedullary tumours, 57% had intraforaminal tumours (dumbbell), and 33% had extradural tumours.<sup>9</sup> Common abnormalities include enlargement of  $\geq 1$  neural foramina secondary to the exiting neurofibroma along the nerve root (dumbbell tumour - Fig. 7). Rarely, it may be caused by dural ectasia (Figs 8a - c), arachnoid cysts or lateral thoracic meningoceles. Posterior scalloping of the vertebral bodies is only due to dural dysplasia (Fig. 8a).<sup>4</sup>

Other abnormalities include kyphoscoliosis (Fig. 9) which may be due either to vertebral anomalies or to large meningoceles or neurofibromas distorting and eroding the adjacent spine and ribs (Fig. 9b). Meningoceles can be lateral or anterior thoracic or anterior sacral in localisation.<sup>4,10</sup>

Intramedullary tumours are typically low-grade astrocytomas. Hamartomatous lesions similar to those seen in the paraventricular white matter are noted with the same MRI signal characteristics.<sup>4</sup>

### Chest

Numerous well-defined subcutaneous neurofibromas may be seen projected over the chest wall (Fig. 10a). Twisted ribbon ribs (Fig. 10b) is a frequently noted feature in NF1, due to mesodermal bone dysplasia. Progressive interstitial fibrosis in the lower zones, and large thin-walled bullae in the upper lung zones, may be seen on chest radiography and high resolution computed tomography (HRCT) of the lungs (Figs 11a and b). Other findings include lateral or anterior thoracic meningoceles presenting as mediastinal masses (Figs 12a and b), paraspinal neurofibromas or neurogenic tumours. Pedunculated intercostal neurofibromas may be confused with lung nodules.<sup>11</sup>

### Musculoskeletal system

The commonly noted abnormalities include marked anterolateral bowing of the tibia/fibula; pseudoarthrosis (Fig. 13a); and atrophic, thinned (Fig. 13b) or absent fibulas, radius and ulna. Subperiosteal haemorrhage with easy detachment of the periosteum from the bone and endosteal sclerosis (Fig. 14a) may also be seen. Intramedullary longitudinal streaks of increased density, multiple non-ossifying fibromas, intraosseous neurofibromas (Fig. 14b), and single or multiple bone cysts (deossification/nonossification) may also be seen. Focal gigantism in the form of a digit or an entire limb is often observed (Figs 15a and b), and also, at times, bone erosion from an adjacent neurofibroma can be observed (Fig. 15c). Plexiform neurofibroma of the skin may cause focal enlargement of an area called a pachydermatocoele<sup>1</sup> (Figs 16a and b).

Large soft-tissue skin neurofibromas can at times cause pressure erosion of the adjacent bone (Figs 16c and d) or may also erode the terminal tufts, mimicking acroosteolysis due to other conditions (Fig. 17).

### Gastrointestinal tract

Solitary neurofibroma, neuroma, ganglioneuroma and schwannoma may present as submucosal or subserosal filling defects, with mass effect on adjacent bowel loops with signs of obstruction. Multiple leiomyomas have also been noted.<sup>10</sup>

### Genitourinary system

Plexiform neurofibromas may compress the renal arteries causing stenosis and secondary hypertension. A urinary bladder mass arising from vesicoprostatic or urethrovaginal plexus may also be seen.<sup>10</sup>

### Vascular lesions<sup>10</sup>

Vascular abnormalities in NF1 include progressive cerebral artery occlusions, aneurysms, vascular ectasia, arterio-venous fistulas and malformations, renal artery stenosis and a high incidence of coarctation of the aorta

### Endocrine abnormalities<sup>10</sup>

NF1 patients also present with visceral and endocrine tumours such as pheochromocytomas and thyroid cancers.

### Associations

The following are associated with NF1:

- multiple endocrine abnormalities (MEA) Type II B
- congenital heart disease (CHD), pulmonary valve stenosis, atrial septal defect (ASD), ventricular septal defect (VSD) and idiopathic hypertrophic subaortic stenosis (IHSS).
- associated congenital abnormalities, failure of vertebral segmentation (Fig. 7a), spina bifida, congenital dislocation of the hip, and osteomalacia due to disturbance of renal function.

### Complications

Malignant transformation to neurofibrosarcomas (Figs 18 a and b) and malignant schwannomas is extremely rare.

In general, imaging cannot distinguish between benign and malignant nerve sheath tumours with certainty; <sup>67</sup>Ga scintigraphy has been shown by Levine *et al.*<sup>12</sup> to be a promising screening technique to identify lesions with malignant degeneration.

## Neurofibromatosis type 2 (NF2)

NF2 is an autosomal dominant condition affecting 1:50 000 people, with the mutation occurring on chromosome 22; cutaneous manifestations are rare as it affects Schwann cells and meninges. The diagnostic criteria are:

- bilateral acoustic neuromas
- first-degree relative with NF2
- single 8th nerve mass or any 2 of the following: schwannoma, neurofibroma, meningioma (often multiple – Figs 19a - c), glioma or juvenile posterior subcapsular lenticular opacity.<sup>4</sup>

## Discussion

NF2 is associated with tumours of the Schwann cells and meninges. Bilateral acoustic neuromas and multiple schwannomas of other cranial nerves are highly suggestive of NF2. Meningiomas are usually multiple<sup>4</sup> (Figs 19a - c).

The acronym MISME characterises NF2 and describes multiple intracranial schwannomas, meningiomas and ependymomas<sup>5</sup> (Figs 20a - c). Other findings include non-neoplastic intracranial calcifications of the choroid plexus,<sup>4</sup> cerebellar and cerebral cortex and occasionally on the surface of the cerebral cortex, spinal cord ependymomas, multiple-

level bulky schwannomas of exiting roots, secondary changes in the spine (expansion, erosions secondary to cord/root tumours) and rarely endobronchial neurofibromas that can cause obstructive bronchiectasis.<sup>13</sup> In the spine, the presence of multiple tumours of various histological types is highly suggestive of NF2.

## Conclusion

Neurofibromatosis, with its multi-faceted presentation, is an entity that has long intrigued and fascinated radiologists, and continues to do so. It is always a diagnostic possibility that should be borne in mind in unusual and rare clinical and radiological presentations.

### Acknowledgements

We thank Dr Z Ebrahim for his contribution of the MRIs of the plexiform neurofibroma of the foot and dumbbell tumour of the spine, and Professor ZI Lockhat for her valued input.

1. Murray RO, Jacobson HG, Stoker DJ. *The Radiology of Skeletal Disorders*. 3rd ed. Philadelphia, USA: Churchill Livingstone, 1990:784.
2. Sutton D. *A Textbook of Radiology and Imaging*. 7th ed. Philadelphia, USA: Churchill Livingstone, 2003.
3. Klatte EC, Edmund A, Franken MD, Smith JA. The radiographic spectrum of neurofibromatosis. *Semin Roentgenol* 1976; XI(1): 17-33.
4. Osborn AG. *Diagnostic Neuroradiology*. 1st ed. Philadelphia, USA: Mosby, 1994: 430.
5. Kornreich L, Blaser S, Shuper A, *et al.* Optic pathway glioma: Correlation of imaging findings with the presence of neurofibromatosis. *Am J Neuroradiol* 2001; 22: 1963-1969.
6. Imes RK, Hiyt WF. Magnetic resonance imaging signs of optic nerve gliomas in neurofibromatosis I. *Am J Ophthalmol* 1991; 111: 729-734.
7. Osborn AG. *Diagnostic Imaging: Brain*. 1st ed. Salt Lake City, USA: Amirsys, 2007: 78-82.
8. Sevicik RJ, Barkovich AJ, Edwards MS, Koch T, Berg B, Lempert T. Evolution of white matter lesions in neurofibromatosis type 1: MR findings. *Am J Roentgenol* 1992; 159: 171-175.
9. Thakkar SD, Feigen U, Mautner V-F. Spinal tumors in neurofibromatosis type 1: a study of frequency, multiplicity and variety. *Neuroradiol* 1999; 41: 625-629.
10. Dähnert W. *Radiology Review Manual*. 5th ed. Philadelphia, USA: Lippincott Williams and Wilkins, 2003: 309-312.
11. Hansell DM, Armstrong P, Lynch DA, Page McAdams H. *Imaging of Diseases of the Chest*. 4th ed. Philadelphia, USA: Mosby, 2005: 679.
12. Levine E, Huntrakoon M, Wetzel LH. Malignant nerve sheath neoplasms in neurofibromatosis: distinction from benign tumours by using imaging techniques. *Am J Roentgenol* 1987; 149: 1059-1064.
13. Mautner VF, Tatagiba M, Lindenau M, *et al.* Spinal tumours in patients in neurofibromatosis type 2: MR imaging study of frequency, multiplicity and variety. *Am J Roentgenol* 1995; 165: 951-955.
14. Kritzing HG. Neurofibromatosis type 2 – a case study. *South African Journal of Radiology* 2002; 6(2): 37-40.
15. Sher BJ, Duncan IC. Neurofibromatosis type 1 – some cranial and spinal manifestations. *South African Journal of Radiology* 2004; 8(3): 32-35.
16. Grobelaar M, George R, Theron SH, Mapukata A, Andronikou S. Neurofibromatosis I (NF1): features on MRI. *South African Journal of Radiology* 2006; 10(4): 33-36.

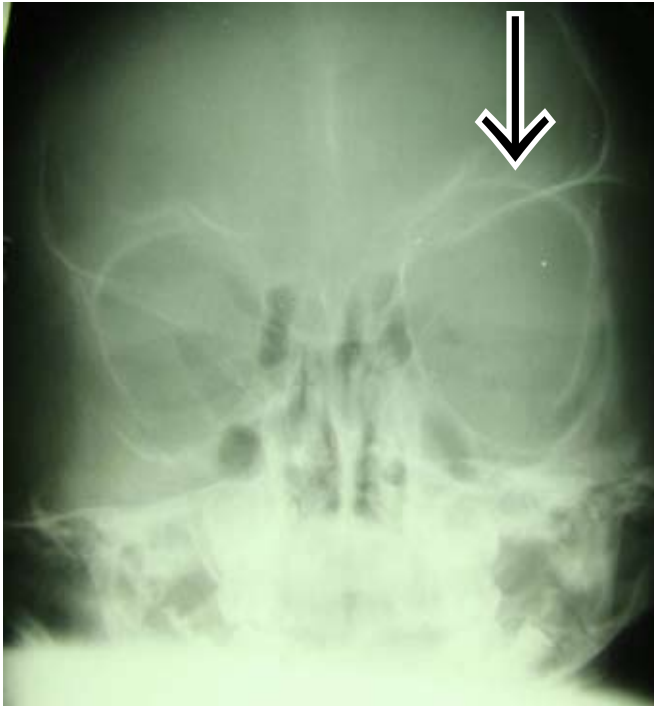


Fig. 1. Frontal X-ray of the skull showing harlequin appearance of the left orbit owing to hypoplasia of the greater wing of the sphenoid bone.



Fig. 2b. Contrast-enhanced axial brain CT with right lambdoid suture defect with an overlying plexiform neurofibroma.



Fig. 2a. Lateral skull X-ray demonstrates defect in the lambdoid suture.



Fig. 2c. Another patient with a large parietal defect.



Fig. 2d. Coronal sutural defect – less commonly seen.

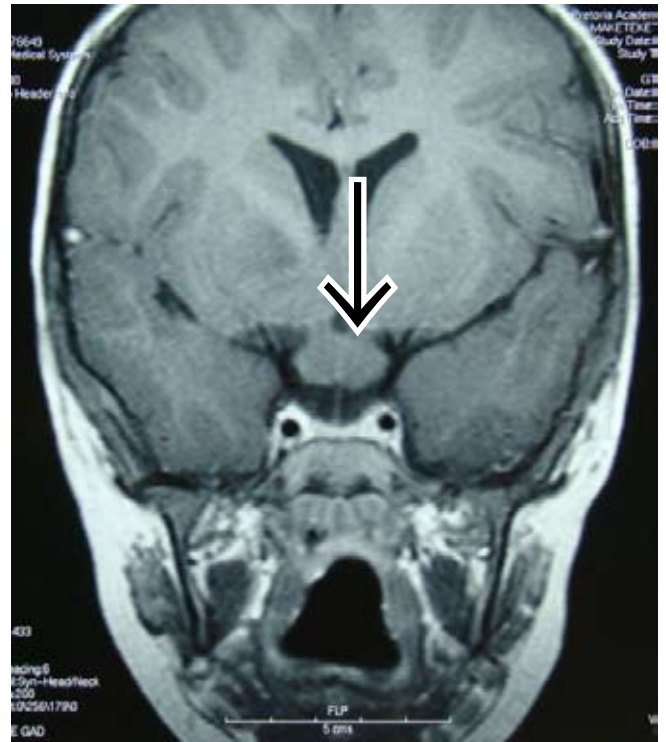


Fig. 3b. Coronal T1-weighted MRI demonstrates chiasmatic glioma in a patient with NF1.

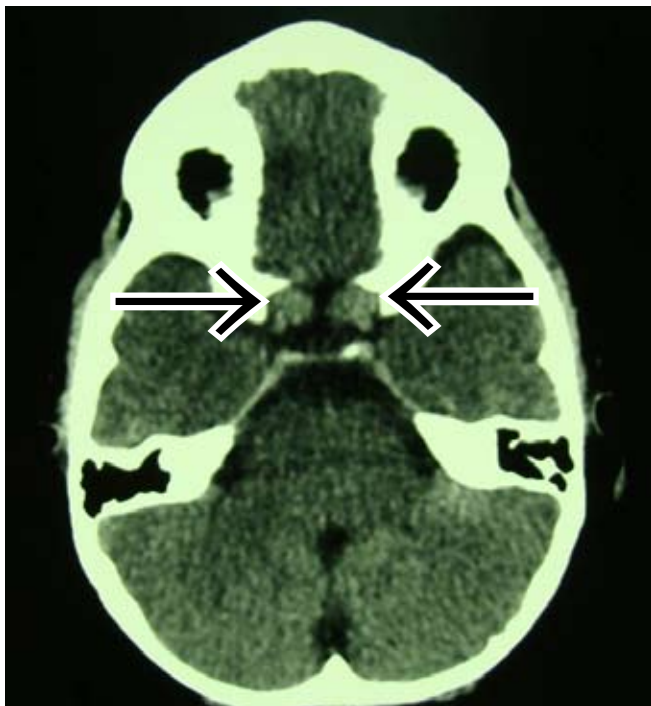


Fig. 3a. Axial non-enhanced brain CT showing bilateral gliomas at the level of the optic nerve extending into the chiasm.

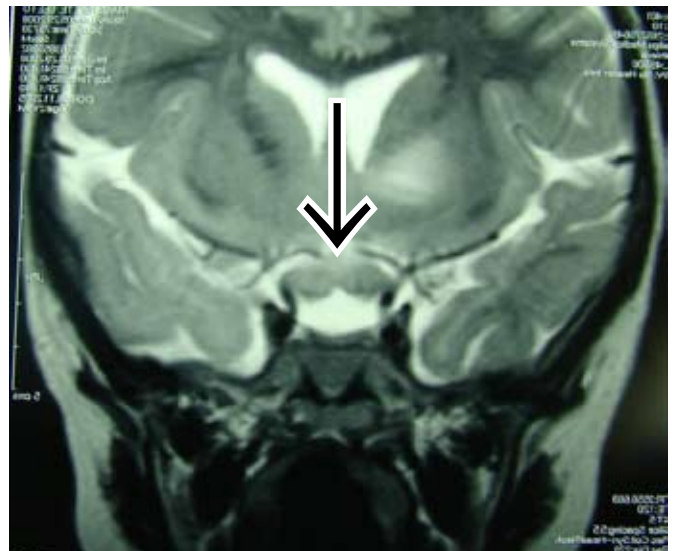


Fig. 3c. Coronal T2-weighted MRI demonstrates chiasmatic glioma in a patient with NF1. High signal is also visualised in the left basal ganglia.

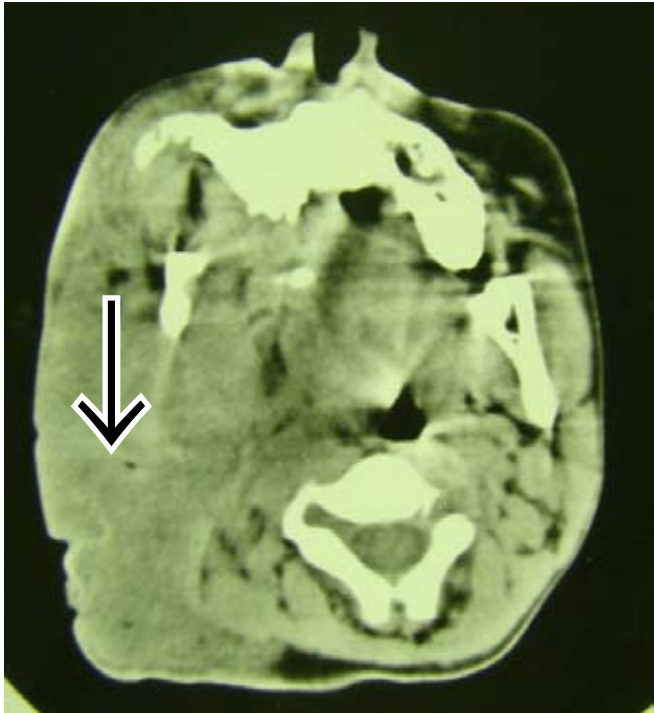


Fig. 4. Axial CT scan of the skull base showing a large plexiform neurofibroma on the right – note the characteristic poorly delineated diffusely infiltrating mass.

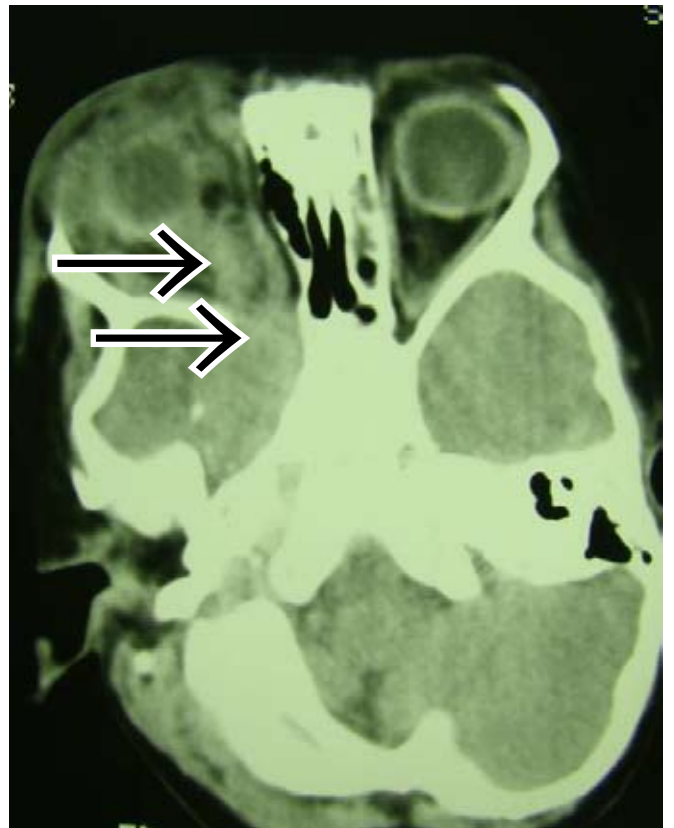


Fig. 5b. Axial non-enhanced brain CT showing plexiform neurofibroma of the right trigeminal nerve, optic glioma and partial hypoplasia of the greater wing of the sphenoid bone.



Fig. 5a. Coronal T1-weighted image of the distal lower limb showing poorly delineated multiple tortuous worm-like masses typical of a plexiform neurofibroma (courtesy of Dr Z Ebrahim).

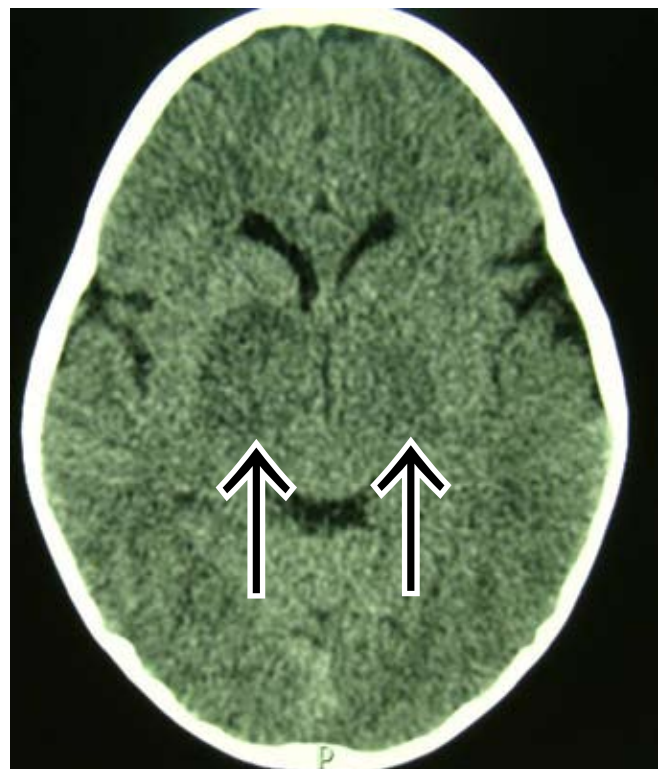


Fig. 6a. Axial non-enhanced brain CT demonstrating bilateral low-density lesions in the basal ganglia with no appreciable mass effect.



Fig. 6b. Axial FLAIR sequence of the same patient as above shows bilateral hamartomatous high signal changes in the basal ganglia (FASI) with no appreciable mass effect.



Fig. 6d. Axial FLAIR MRI sequence demonstrating bilateral optic nerve gliomas and FASI changes in the brainstem.

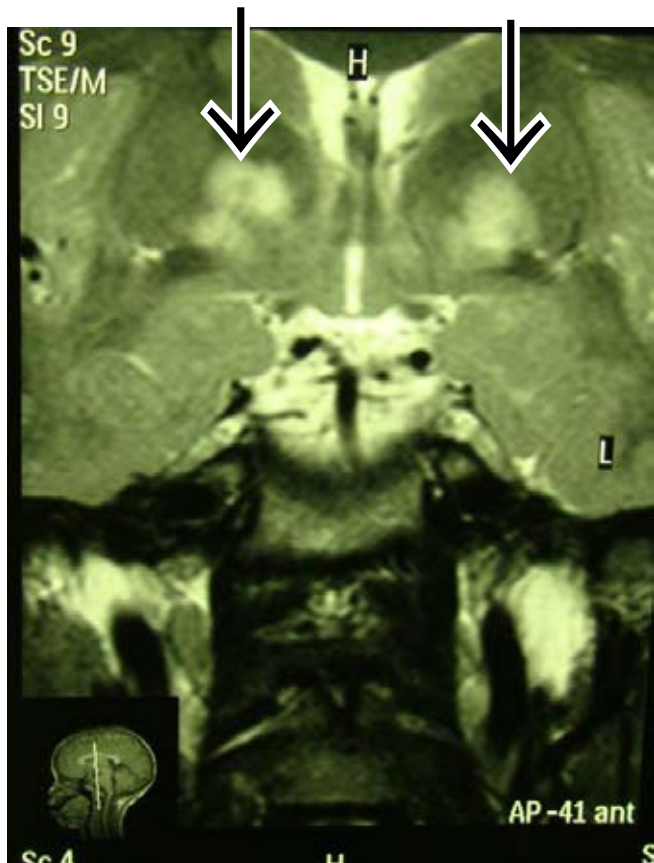


Fig. 6c. Coronal T2-weighted MRI of the same patient. Note that these lesions are hyperintense with fairly well-defined margins and no mass effect.

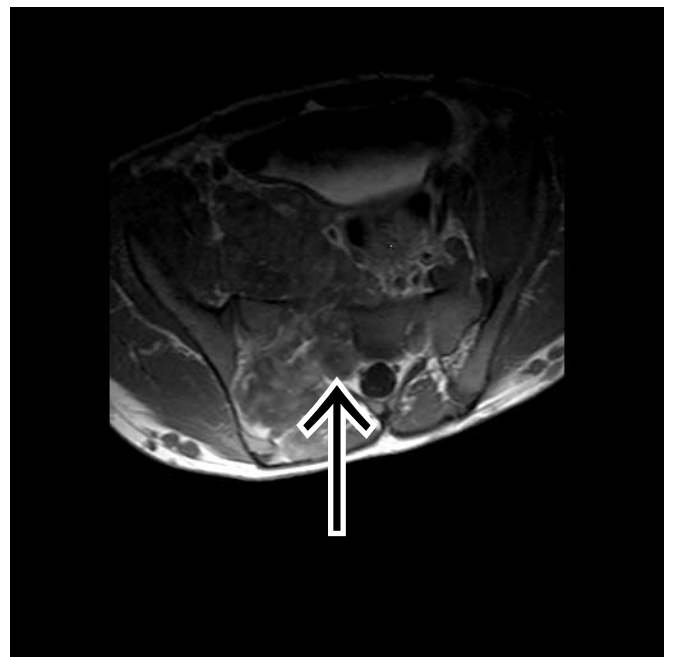


Fig 7a.

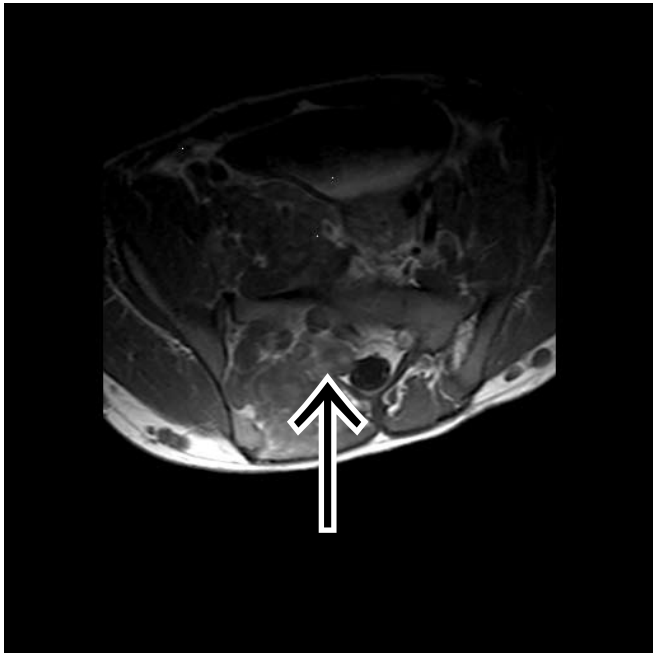


Fig 7b.

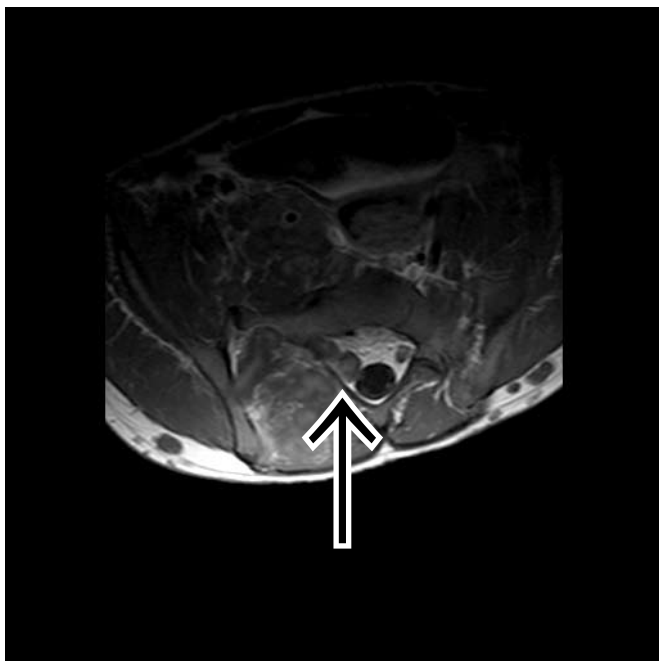


Fig. 7c. Axial T1-weighted MRI of the lumbar spine showing exiting neurofibroma along the nerve root at the level of the sacral nerve (courtesy of Dr Z Ebrahim).

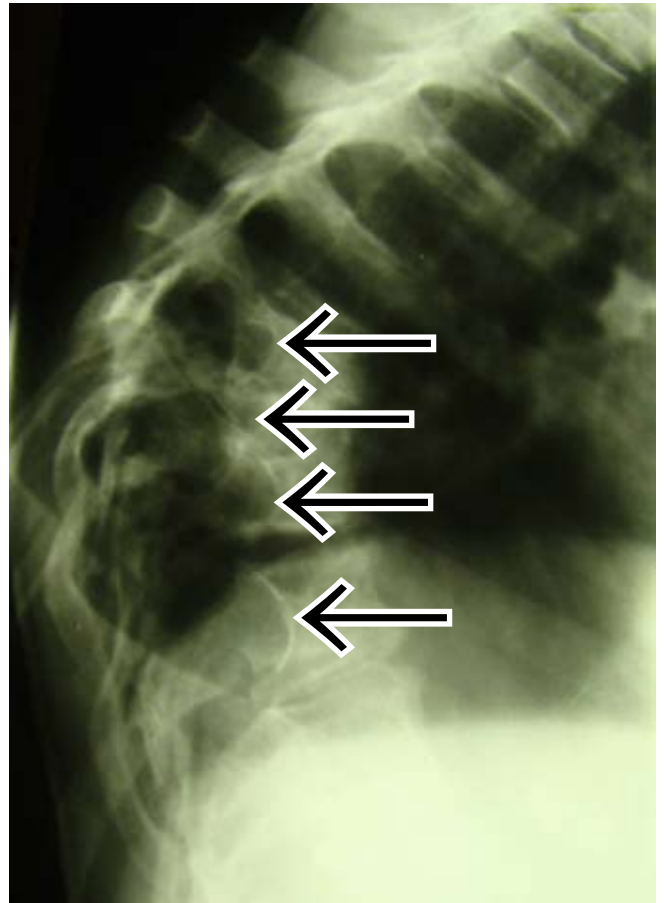


Fig. 8a. Lateral X-ray of the thoracic spine showing enlargement of the neural foramina at multiple levels and posterior vertebral scalloping gibbus owing to multiple dumbbell tumours and dural ectasia.



Fig. 8b. Myelogram of the lumbar spine in a different patient showing multilevel vertebral anomalies and dural ectasia.



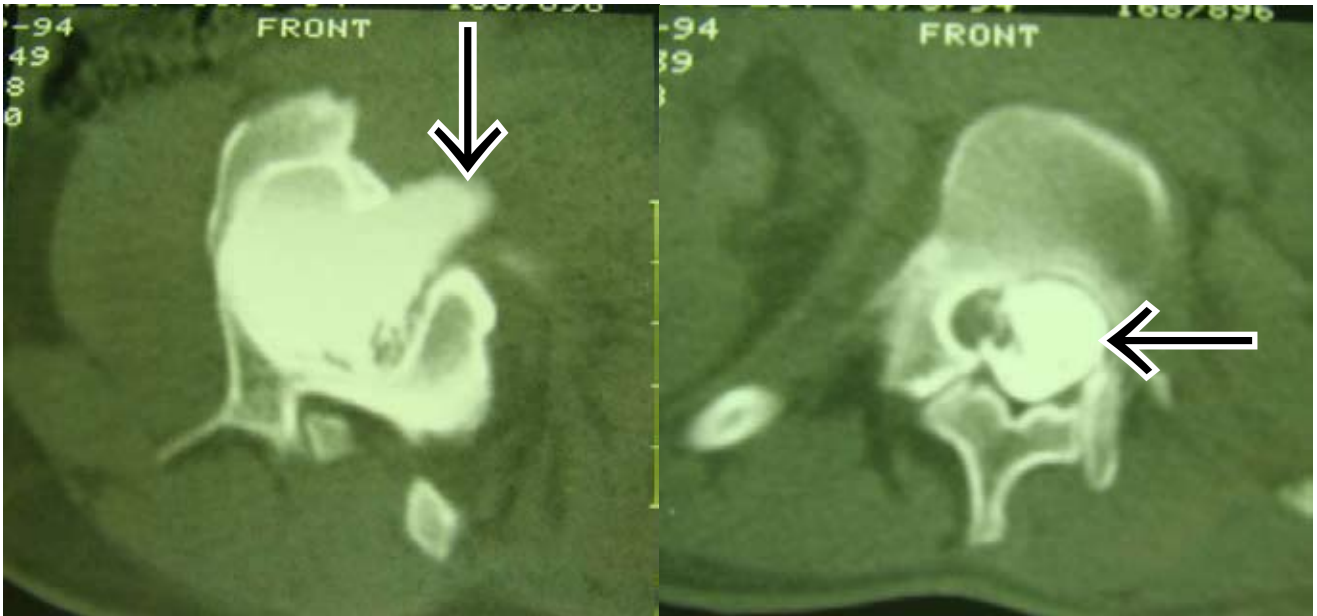


Fig. 8c. CT myelogram of the same patient as in 8b with dural ectasia.

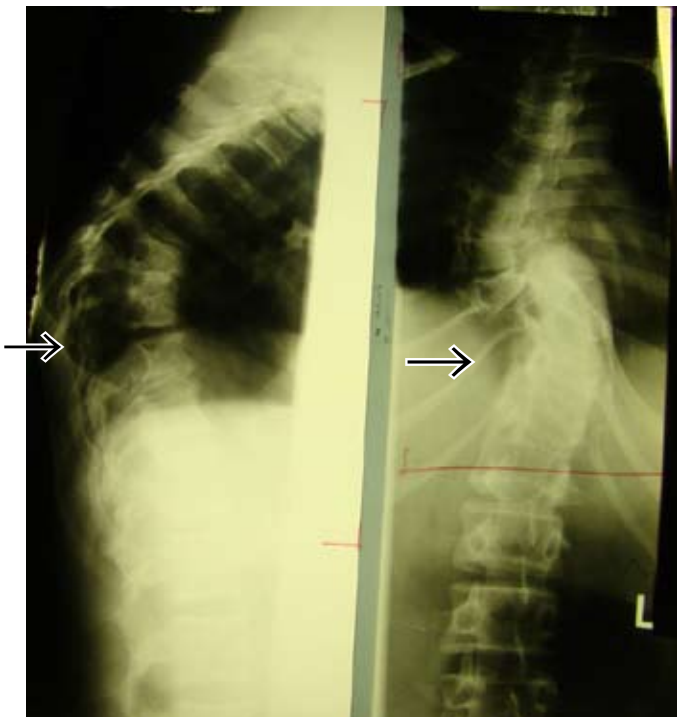


Fig. 9a. Lateral and frontal X-rays of the thoracic spine demonstrating kyphoscoliosis, which may be due either to vertebral anomalies or to large meningoceles or neurofibromas.

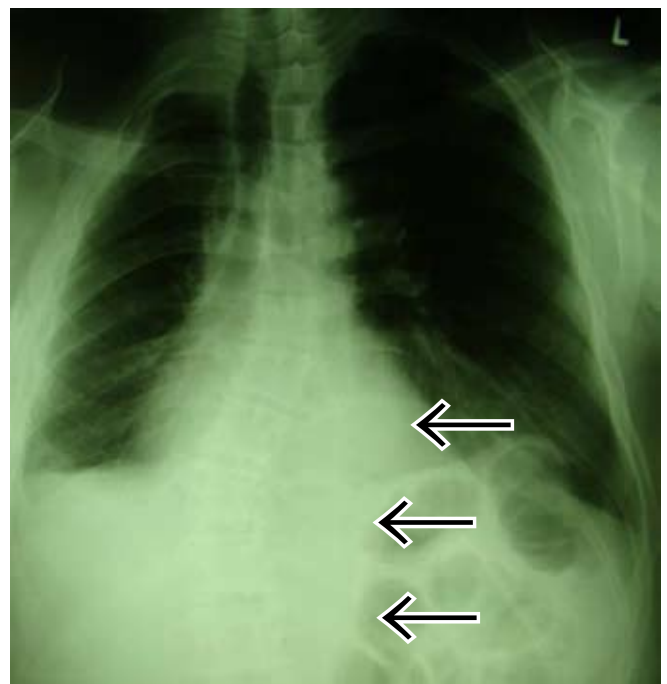


Fig. 9b. Frontal chest X-ray demonstrates dextroscoliosis of the lower thoracic spine associated with large soft-tissue left para-vertebral mass, erosion and thinning of the 10th, 11th and 12th ribs on the left, and left lateral vertebral body scalloping.



Fig. 10. CT scan of the preceding patient showing a large plexiform neurofibroma on the left side, causing spine and rib changes.

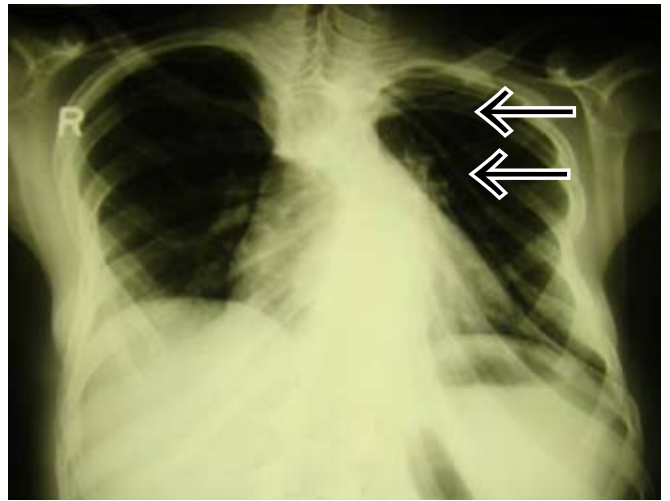


Fig. 10b. Chest X-ray showing twisted ribbon ribs.

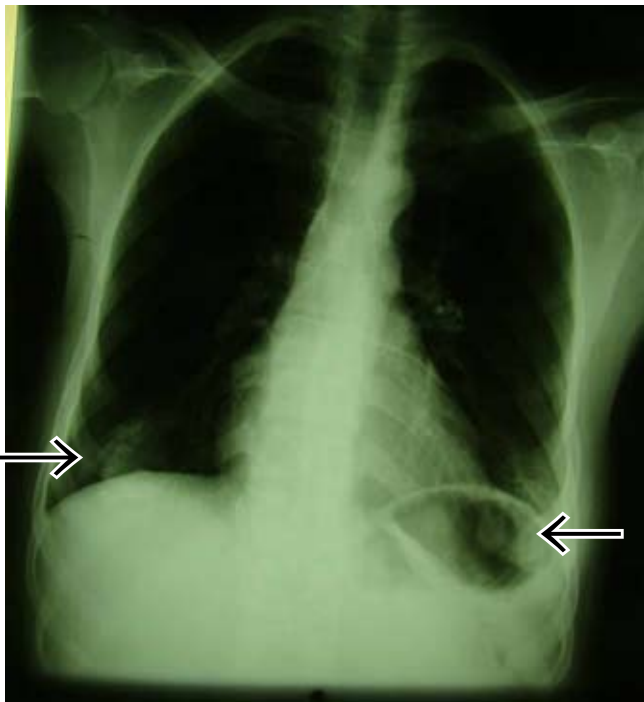


Fig. 10a. Frontal chest X-ray showing bilateral cutaneous neurofibromas of the areola projecting over the lung fields.

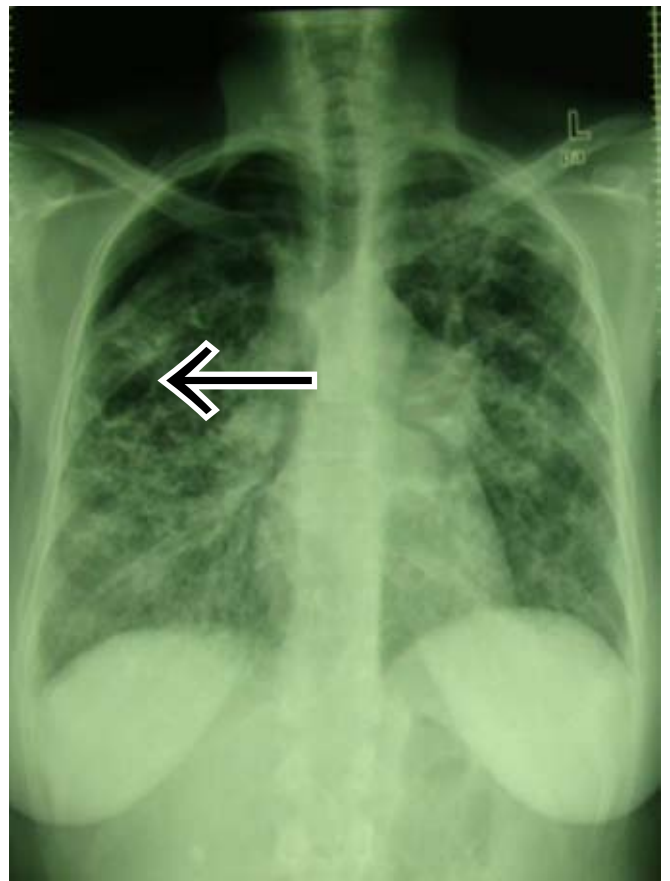


Fig. 11a. Frontal chest X-ray with interstitial fibrosis of NF1 complicated by spontaneous pneumothorax on the right.

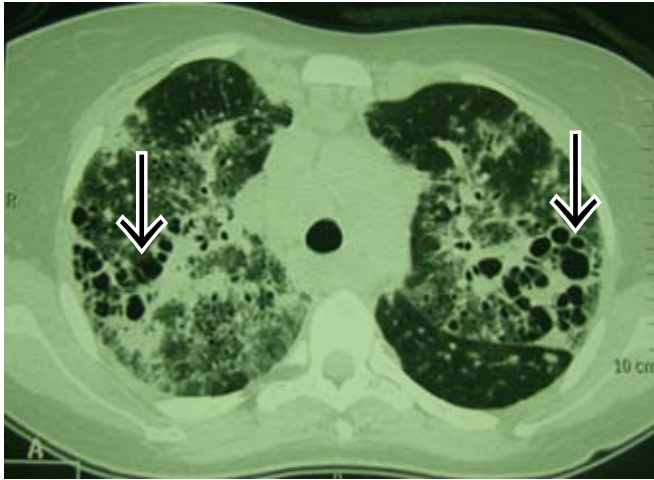


Fig. 11b. Axial HRCT of the same patient showing interstitial fibrosis and cystic changes.

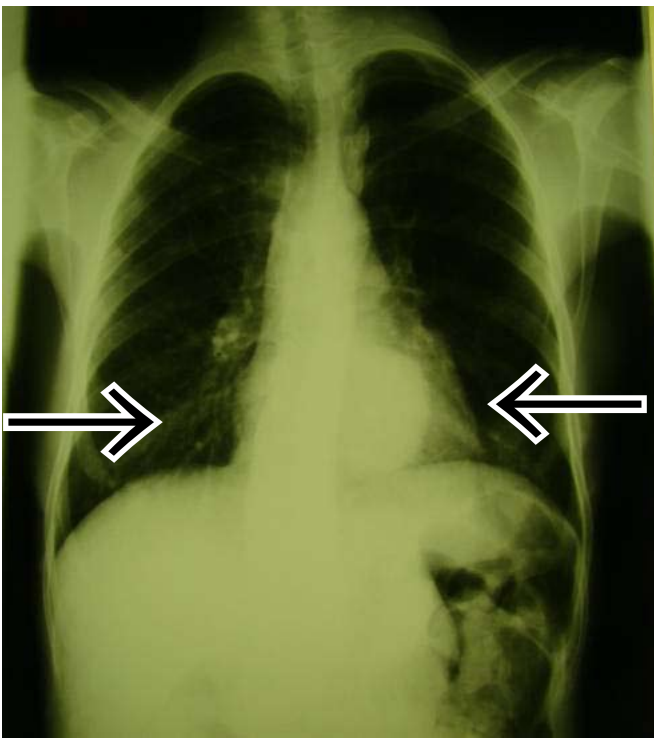


Fig. 12a. Frontal chest X-ray showing multiple cutaneous neurofibromas projecting over the lung fields and a posterior mediastinal mass on the left.



Fig. 12b. CT myelogram in the same patient demonstrating postero-lateral meningocele.



Fig. 13a. Patient with NF1 presenting with radial fractures. Note also pseudoarthrosis of the ulna.



Fig. 13b. Anteroposterior X-ray of the forearm with thinned atrophic distal radius.



*Fig. 14a. Anteroposterior X-ray of the proximal tibia and fibula demonstrating endosteal sclerosis of the tibia and an intraosseous neurofibroma of the fibula with associated soft-tissue mass.*



*Fig. 14b. Anteroposterior radiograph of the knee with intraosseous neurofibroma of the proximal tibia.*



Fig. 15a.



Fig. 15b. Frontal and lateral radiographs of the right foot showing macrodactyly (focal gigantism) of the 4th and 5th toes.



Fig. 15c. Posteroanterior X-ray of the chest with bilateral soft-tissue neurofibromas eroding the lateral ends of the clavicle.



Fig. 16a. Frontal X-ray of the hands showing large plexiform neurofibroma causing focal enlargement, elongation, thinning of the metacarpals and pressure changes (scalloping) of the bases of the metacarpals and carpal bones, also called a pachydermatocoele.

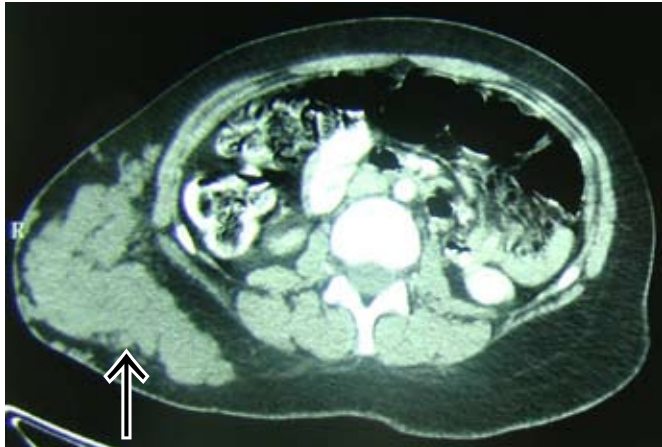


Fig. 16b. CT scan of a different patient with a large right plexiform neurofibroma causing distortion of the abdominal wall.



Fig. 16d. Lateral view of the cervical spine with a large anterior soft-tissue neurofibroma causing pressure erosion of the anterior margin of C3.



Fig. 16c. Anteroposterior X-ray of the knee with soft-tissue neurofibroma of the knee with extensive pressure changes.



Fig. 17. Frontal X-ray of the terminal tufts with acroosteolysis owing to an overlying neurofibroma.



Fig. 18a.



Figs 18a and b. Posteroanterior and lateral X-rays of the chest with sarcomatous change in the right posterior mediastinal neurofibroma with rib erosions. Note surgical clips (arrowed) in the neck from previous surgery.

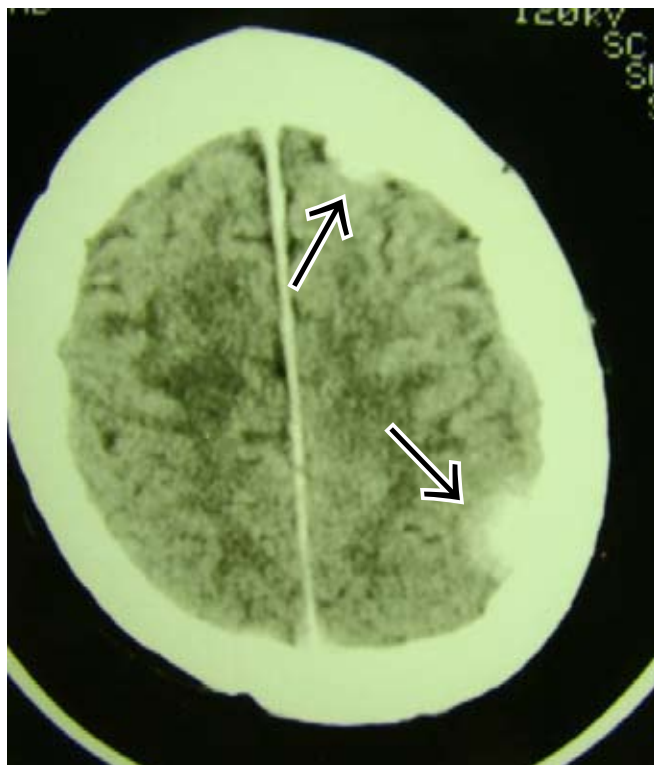


Fig. 19a.

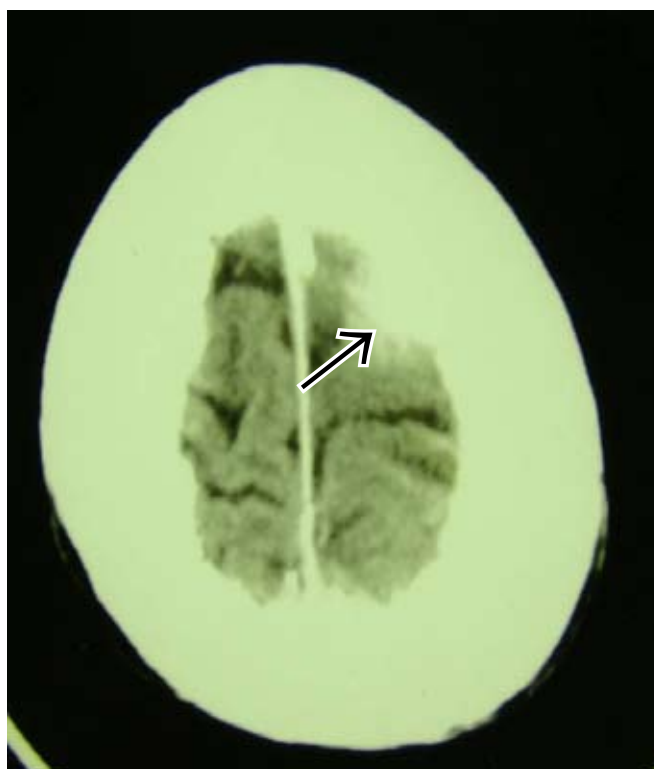


Fig. 19b.





Fig. 19c. Axial contrast-enhanced brain CT at multiple levels with multiple meningiomas and bilateral acoustic neuromas.

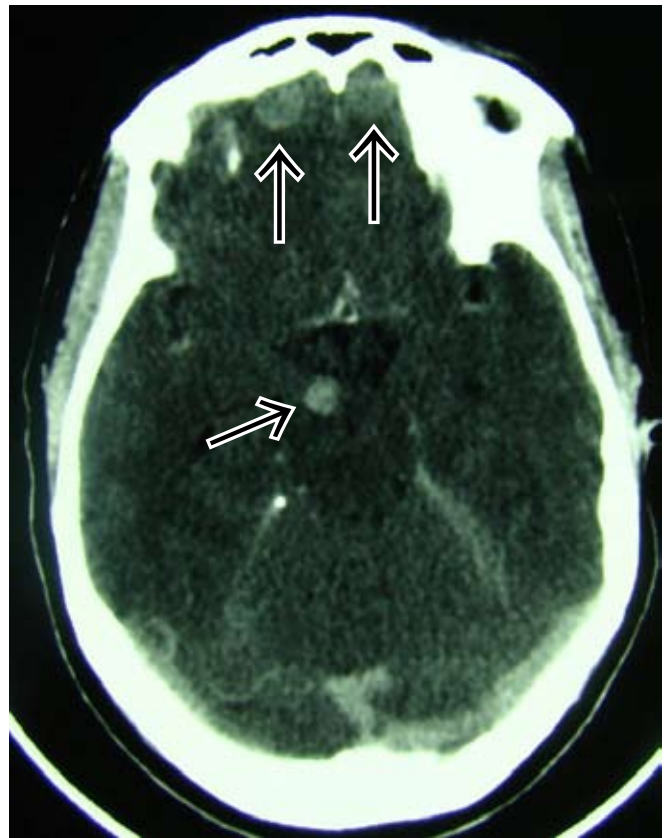


Fig. 20b.



Fig. 20a.

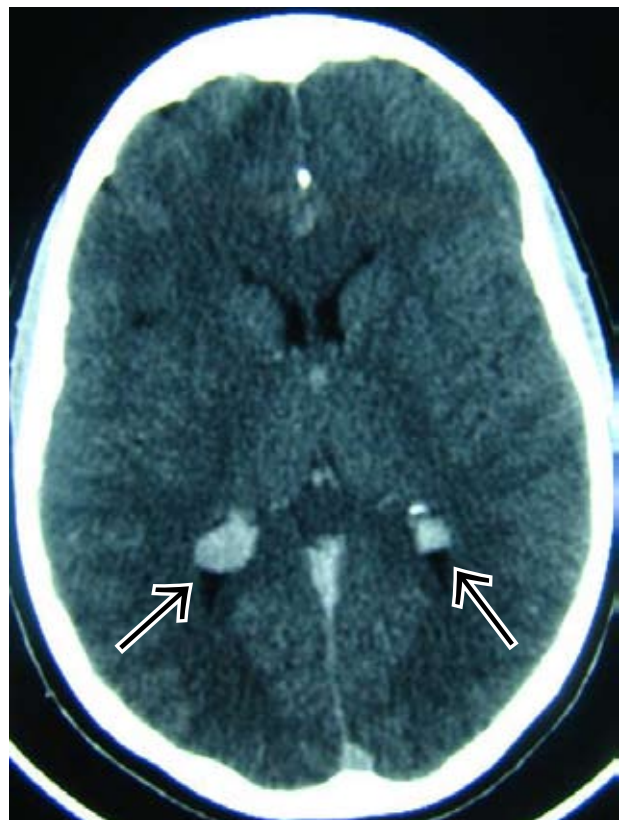


Fig. 20c. Axial contrast-enhanced CT scans at different levels showing multiple intracranial schwannomas (acoustic), meningiomas, and ependymomas of the lateral ventricles (MISME). Note also in Fig. 20a an abnormally tortuous optic nerve on the right.